An Experimental Study of Scale-up, Oxidant, and Response Characteristics in PEM Fuel Cells

Kap-Seung Choi, *Member, IEEE*, Jiwoong Ahn, *Member, IEEE*, Jungkoo Lee, *Member, IEEE*, Nguyen Duy Vinh, *Member, IEEE*, Hyung-Man Kim, *Member, IEEE*, Kiwon Park, *Member, IEEE*, and Gunyong Hwang, *Member, IEEE*

***Abstract*—It is important for fuel cell to become flexible in order to accommodate the situations of application areas for reducing costs and expanding coverage. Scale ups in series and parallel to 1-kW class proton exchange membrane (PEM) fuel cell stack are characterized experimentally with oxidant as air and oxygen. Through a serial scaled-up 4-cell stack with an active area of 25 cm^2 and a parallel scaled-up single cell with an active area of 100 cm^2, respectively, the 1-kW class 20-cell stack with an active area of 150 cm^2 per cell is scaled up from the basic unit cell with maintaining their performances. The polarization and power curves of the 1-kW class PEM fuel cell stack with the reactants H_2/air and H_2/O_2 are evaluated. Sufficient power of the PEM fuel cell can operate at flexible nominal current of 40–80 A and nominal voltage of 12–15 V for providing durability and balance between cells. The 1-kW class PEM fuel cell stack is characterized through the comparison of cell voltage differences utilizing H_2/air and H_2/O_2. Both cell voltages with H_2/air and H_2/O_2 follow well the one-twentieth of the responding stack voltages with the small difference.**

***Index Terms*—Design for experiments, fuel cells, performance analysis, power measurement.**

I. Introduction

FUEL CELLS technology has been prompted as a very active research field because the need of the hour is power generation with environment throughout the world. The proton exchange membrane (PEM) fuel cells, which directly convert the chemical energy of hydrogen into electrical energy, are one of the most promising alternative power sources for transportation, portable electronics, and stationary applications [1]. Fuel cell systems are available to meet the needs of applications ranging from portable electronics to utility power plants. The overall system is efficient at full- and part-load, scalable to a wide range of sizes, environment friendly, and potentially competitive with conventional technology [2].

Under normal operation, a simple fuel cell typically produces 0.5–0.9 V. For use in energy generation systems, where a relatively high power is needed, several cells are connected in series, arranging a stack that can supply hundreds of kilowatts [3]. One of the key challenges of fuel cell systems is the appropriate media supply, heat management, and operation management in order to realize stable operation for transportation, portable electronics, and stationary applications. During the design phase, the power converter needs to be tested and adjusted with the real-fuel cell stack, and then, it must be validated [4]. PEM fuel cells show some losses of efficiency and power density with scale-up in the area of the electrodes and the increase in number of cells in a stack. The main reason for this is that removal of the product, liquid water, becomes more difficult in larger systems; furthermore, a high water vapor pressure in the reactant flows causes an increase in overpotential, especially at the cathode. A problem strongly related to water management is that of thermal management in stacks [5].

The fuel cells produce electricity from a simple electrochemical reaction, in which an oxidant and a fuel react to form a product, which is water for the typical fuel cell. The fuel is typically hydrogen (H_2), and the oxidant is usually the oxygen (O_2) from air. The O_2 or air continuously passes over the cathode and the H_2 passes over the anode to generate electricity, by-product heat and water [6]. The cathode flooding with H_2/air increases the O_2 mass transfer resistance in the electrode and the degrees of hysteresis in the polarization and power density with H_2/air become worse than those with H_2/O_2. O_2 is transported across the cathode gas diffusion layer (GDL) by a combination of pressure-driven convection through the porous GDL and concentration-driven diffusion. Because the vapor in the cathode gas flow channel is saturated with water vapor, additional water produced at the cathode must be immediately condensed. When oxygen is consumed at the cathode catalyst layer (CL), there is a reduction of the total pressure due to the reduction in the total number of moles in the vapor [7].

In this paper, the 1-kW class 20-cell PEM fuel cell stack with an active area of 150 cm^2 is scaled up both in series and parallel, and characterized experimentally with air and O_2 as oxidant. Scale-up was started from the basic unit cell whose serpentine flow field was characterized geometrically to enhance the performances in relation to pressure drop, discharge of condensed water, maximization of cell voltage, and uniformity

Manuscript received October 25, 2013; revised March 28, 2014, February 18, 2014, and January 16, 2014; accepted December 30, 2013. Date of publication May 30, 2014; date of current version August 18, 2014. This work was supported in part by a National Research Foundation of Korea grant funded by the Korean government (MEST) under Grant number 2009-0080496, and in part by the New & Renewable Energy of the Korea Institute of Energy Technology Evaluation and Planning grant funded by the Korea government Ministry of Knowledge Economy under Grant number 2012T100100660. Paper no. TEC-00631-2013.

K.-S. Choi is with the Department of Automobile Engineering, Tongmyong University, Busan 608-711, Republic of Korea (e-mail: kschoi@tu.ac.kr).

J. Ahn, J. Lee, N. D. Vinh, and H.-M. Kim are with the Department of Mechanical Engineering & High Safety Vehicle Core Technology Research Center, Inje University, Gyongsangnam-do 621-749, Republic of Korea (e-mail: ljk2866@naver.com; auvwm@nate.com; vinh.nguyenduy@hust.edu.vn; mechkhm@inje.ac.kr).

K. Park and G. Hwang are with the Department of Green Automobile Engineering, Youngsan University, Gyongsangnam-do 626-790, Republic of Korea (e-mail: kiwonp@hotmail.com; gyhwang@ysu.ac.kr).

Color versions of one or more of the figures in this paper are available online at http://ieeexplore.ieee.org.

Digital Object Identifier 10.1109/TEC.2014.2322877

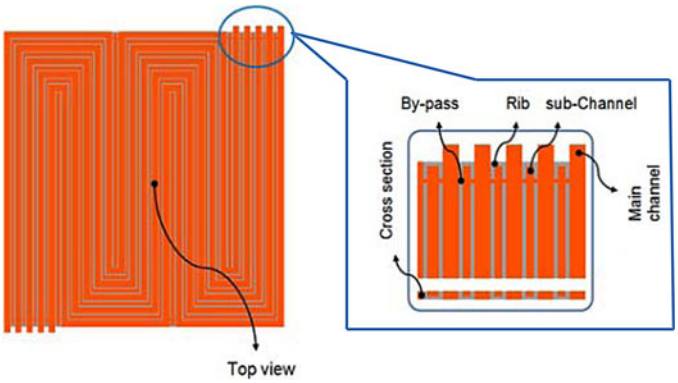

Fig. 1. Schematic diagram of the serpentine flow-field with subchannels and by-passes.

of current density over the active area of 25 cm^2 [9]. Based the previous geometrical characterization results, we designed a novel serpentine flow field with subchannels and by-passes (SFFSB) to promote under-rib convection, as shown in Fig. 1. The numerical results show that the presence of a convective flow in the under-rib regions enables more effective utilization of electrocatalysts by increasing the reactant concentration and by facilitating liquid water removal in those regions, compared to conventional advanced serpentine flow field (CASFF). For the experimental performance evaluation, the improvement of under-rib convection made a big impact on the vitalization of mass transfer and electrochemical reaction so that it was verified that the performance of SFFSB (0.615 W/cm^2 at 0.47 V) was improved by 23.7% in comparison with CASFF (0.497 W/cm^2 at 0.47 V) [10]–[13]. Compared to CASFF, SFFSB is characterized by low pressure in the entrance, and it finally shows characteristics similar or equal to those of CASFF, by gradually decreasing the pressure rate as reacting gases move closer to the exit. Such a pressure difference occurs because the diffusion of reacting gases becomes smooth as the intensity of under-rib convection is increased by adding subchannels. As the concentration distribution of reacting gases becomes uniform inside a fuel cell, the diffusion of reacting gases improves the uniformity of current density distribution and temperature distribution by electrochemical reaction. There is a little increase of temperature distribution in some parts of the rib because the cooling rate decreases when some parts of the rib gets dry while the flow-field pattern of the under-rib convection moves from the main channels to the subchannels, removing the water created in parts of the rib, into subchannels. Moreover, as the water existing in parts of the rib is removed into subchannels, the anode liquid water mass fraction increases because of the reduced electro-osmotic drag [12]. Based on the previous results, we aim to scale up and test 1-kW class PEM fuel cell that can meet the performances of power, operational reliabilities, and safety requirements with air and O_2 as oxidant.

II. System Description

To establish the scale-up procedure of PEM fuel cells, we have fabricated subsequently a basic unit cell with an active area of 25 cm^2, a serial scaled 4-cell stack with an active area of 25 cm^2, and a parallel scaled-up single cell stack with an active area of 100 cm^2, and serial and parallel scaled-up 1-kW class 20-cell stack with an active area of 150 cm^2, as shown in Fig. 2. A basic unit of 25 cm^2 [11], a serial scaled 4-cell stack, and a parallel scaled-up single cell of 100 cm^2 were evaluated in the previous study, and 1-kW class PEM fuel cell stack is evaluated in this study. All fuel cells have SFFSB to promote under-rib convection. The properties of a membrane electrode assembly (MEA), which is composed of two GDLs, a membrane, and two electrodes, are presented in Table I.

The fuel cell performances are evaluated by the polarization curve measured while adjusting the pressure, temperature, humidity, and flow rates of the reacting gases using the test equipment built at Inje University [11], as listed in Table II. Because the PEM fuel cell performance depends greatly on the operating conditions, the test equipment controlled the operation of the PEM fuel cells carefully and continuously. The test equipment consists of an electronic load, a flow controller, a temperature controller, a relative humidity controller, and a DEWETRON DEWE-30-16 data acquisition system.

Experiments are carried out using the Fuel Cells Testing & Standardisation NETwork (FCTESTNET) performance test procedure [14], which was originally developed under the Research & Training Network. The FCTESTNET performance test procedure is a method used to evaluate the activation loss region, the ohmic resistance loss region, and the mass transport loss region of fuel cells. In the performance tests, the load current is controlled to minimize physical damage to the MEA and to maintain a stable electrical load.

Fuel in the form of H_2 gas is fed into the anode side of the PEM fuel cell. The oxidant in a fuel cell is O_2, either in air or as a pure O_2, which enters the fuel cell through the cathode inlet. The reactant gases H_2 and O_2 flow through channels machined into graphite plates and migrate through GDLs to the catalyst surface on their respective sides of the MEA. Aided by the noble metal catalyst in the anode, H_2 is oxidized to form protons and electrons.

The bipolar plates of the anode and the cathode are produced in the same semicounter flow format; that is, the inlet and the outlet of H_2 are at the top left and the bottom right, respectively, while the inlet and the outlet of O_2 or air are at the top right and the bottom left, respectively. A unique feature of PEM fuel cells compared with other types of fuel cells is that the former feature a solid proton-conducting electrolyte [15]–[18]. The MEA is the "heart" of the PEM fuel cell. In this study, a W.L. Gore & Associates PRIMEA Series 57 MEA is used and sandwiched between anode and cathode SIGRACET GDLs, which have a porous structure. The MEA has a membrane and two electrodes composed of highly dispersed carbon-supported platinum catalysts.

III. Performance Test Results

The initial performance of the fuel cells was greatly affected by the humidification of the MEA, the electrical load, and the abundant supply of the reaction gas. Therefore, sufficient

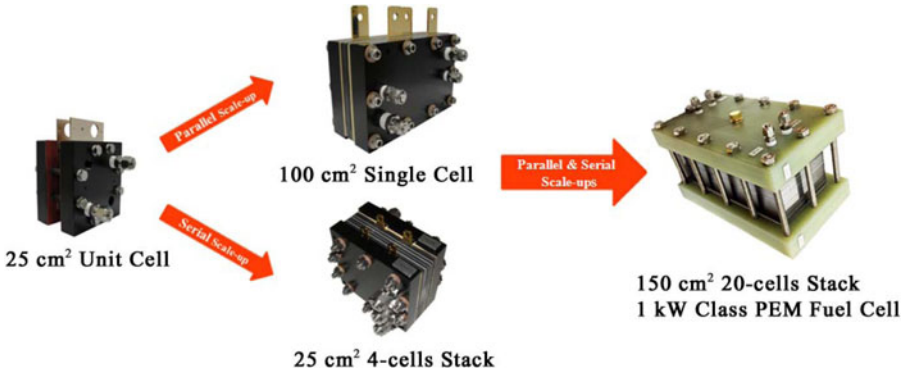

Fig. 2. Photographs of a basic unit of 25 cm^2, a serial scaled 4-cell stack and a parallel scaled-up single cell of 100 cm^2, and 1-kW class PEM fuel cell stack of 20 cells on 150 cm^2 active areas per cell (not to scale).

TABLE I
COMPONENTS AND PROPERTIES OF THE MEA [9]

	MEA[1] components and properties	Values
Electrode	Thermal conductivity (W/m·K)	5.7
GDL		250
	Thickness after compressed (μm)	
	Permeability (m^2)	1.0e–12
	Porosity after compressed (%)	70
	Diffusion adjustment (%)	50
	Thermal conductivity (W/m·K)	0.21
Membrane	Thickness (μm)[2]	50
	Thermal conductivity (W/m·K)	0.15
	Dry membrane density (g/m^3)	2.0
	Equivalent weight of dry membrane (g/mol)	1100
	Cathode transfer coefficient	0.6
	Anode transfer coefficient	1.2

[1]MEA: W.L. Gore & Associates PRIMA Series 57.
[2]including 12.5 12.5 μm Pt CL of 0.4 mg/cm^2.

TABLE II
INLET AND OPERATING CONDITIONS

Inlet conditions at the anode		
Fuel	H_2	
Stoichiometry	1.5	
Inlet temperature (°C)	70	
Inlet humidity (%)	100	
Mass fraction of H_2	0.078	
Inlet conditions at the cathode		
Oxidant	O_2	Air
Stoichiometry	1.5	2.0
Inlet temperature (°C)	70	70
Inlet humidity (%)	100	100
Mass fraction of O_2 and air	0.726	0.169
Operating conditions		
Exit pressure (kPa)	101	
Cell temperature (°C)	70	
Open circuit voltage (V)	0.96	

humidification was induced for 30 min to hydrate the dried MEA prior to measuring cell performance. The experiment was carried out using the FCTESTNET performance test procedure. The results of each test procedure were confirmed by supplemental literature and experiments [11]. We tested the polarization and power density of the 1-kW class PEM fuel cell 20-cell stack with an active area of 150 cm^2 utilizing air and O_2 as an oxidant while the load currents were controlled according to predefined schedules, as shown in Fig. 3.

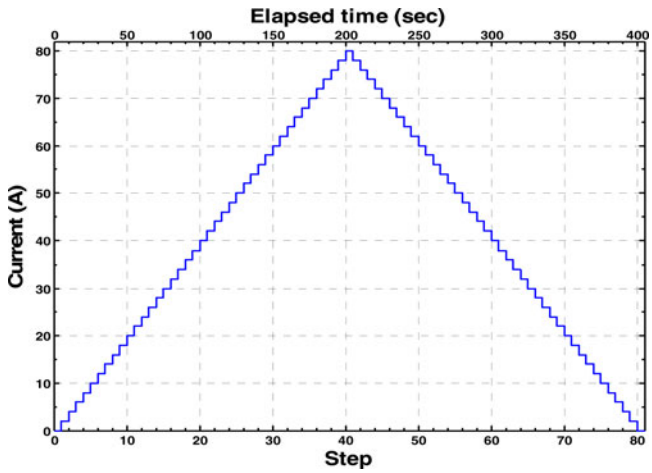

Fig. 3. FCTESTNET maximum performance test procedure of the PEM fuel cell from 0 to 80 A in decrements of 2 A has been processed with 5 s per step.

A. Polarization and Power Curves of the 1-kW Stack

The polarization and power curves of the 1-kW class PEM fuel cell stack with the reactants H_2/air and H_2/O_2 are shown in Fig. 4. The power $P(t)$ is obtained from the voltage $V(t)$ and the current $I(t)$ of the polarization curve as follows:

$$P(t) = V(t) \times I(t). \tag{1}$$

In Fig. 4, there is a hysteresis in the voltage but just invisible in the power with both H_2/air and H_2/O_2 visible because the power is calculated as the product of voltage as well as the same current.

We did not experiment on the entire polarization up to the concentration loss zone and finish the experiment at 80 A because of high current safety in our experimental apparatus. The stack voltage and power are varied with current as follows: the stack voltage and power with H_2/air and H_2/O_2 are similar in

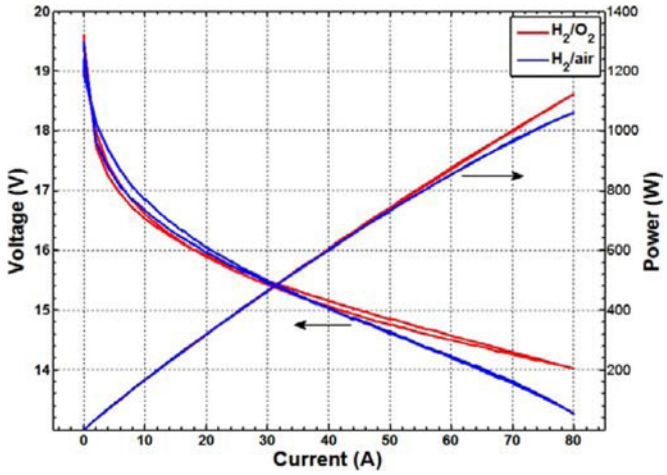

Fig. 4. Polarization and the power density curves of the 1-kW class PEM fuel cell 20-cell stack on 150 cm^2 active areas per cell are compared between the reactants of H_2/air (blue) and H_2/O_2 (red).

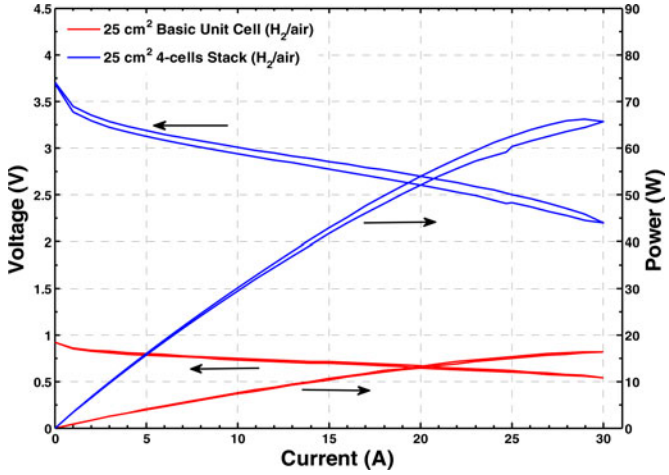

Fig. 5. Comparisons of cell voltage and power density curves between the basic unit cell and the serial scaled-up 4-cell stack with H_2/air.

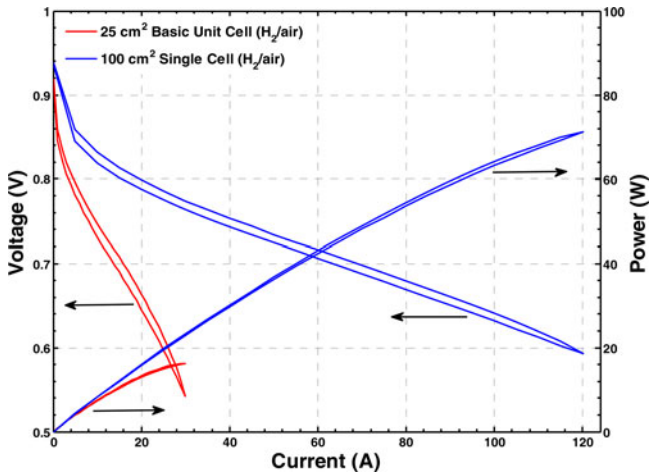

Fig. 6. Comparisons of cell voltage and power density curves between the basic unit cell and the parallel scaled-up single cell with H_2/air.

the load current range of 0 A to approximately 0.2 A, the stack voltage with H_2/O_2 is less than that with H_2/air but the powers with H_2/air and H_2/O_2 are similar in the load current range of 0.2 A to approximately 30 A, the stack voltage with H_2/O_2 is higher than that with H_2/air but the powers with H_2/air and H_2/O_2 are similar in the load current range of 30 A to approximately 50 A, and the stack voltage and power with H_2/O_2 are higher than those with H_2/air in the load current range over 50 A. This means that the mass transport loss with H_2/O_2, which determines the maximum power, is higher than that of H_2/air at mass transport region. These mass transport limitations are the influence of diffusional resistance in the CL causing hindrance to access by nitrogen (N_2) [7], [19]. In the load current range of 0.2 A to approximately 30 A, ohmic resistance with H_2/O_2 is stronger than that with H_2/air. However, over approximately 30 A, voltage due to electrochemical reaction with H_2/O_2 is overproduced considering ohmic resistance and become higher than that with H_2/air.

Fig. 4 presents the maximum powers with the reactants of H_2/air and H_2/O_2 were 1062 and 1122 W, respectively; therefore, the reactants of H_2/O_2 enhanced 5.7% higher maximum power at the same current of 80 A. The previous results with the parallel scaled-up single cell of 100 cm^2 [8] show that as current is increased up to 120 A, maximum power with H_2/O_2 is higher by approximately 20% than that with H_2/air; however, current is limited to 80 A because of the achievement over 1 kW and the balance between 20 cells. The power of PEM fuel cell increases proportionally to the O_2 concentration of oxidant at the cathode [20].

B. Characterization of Scale-up

To achieve the 1-kW class PEM fuel cell, there are two approaches of a serial scaled-up by stacking cell and a parallel scaled-up by increasing active area, as shown in Fig. 1. The comparisons of cell voltage and power density curves from a basic unit cell with an active area of 25 cm^2 to a serial scaled 4-cell stack with an active area of 25 cm^2 and a parallel scaled-up single cell with an active area of 100 cm^2 utilizing H_2/air are given in Figs. 5 and 6, respectively [8]. Two approaches of a serial scaled-up by stacking cell and a parallel scaled-up by increasing active area from 25 to 100 cm^2 have their advantages and disadvantages while maintaining nearly the same power densities with varying voltage and current.

Fig. 5 shows that the maximum cell voltage and the maximum power of the serial scaled 4-cell stack is nearly four times more than those of the basic unit cell. The serial scaled-up by stacking cell has the advantages of safety and compact assembly due to thin and flexible power cable with no increase in current, but the disadvantages of difficult assembly and maintenance due to too many electrically connected cells in series because the performances of individual cells should be maintained by measuring the current of the entire stack and the voltages of individual cells.

Fig. 6 shows that the maximum current and the maximum power of a parallel scaled-up single cell of 100 cm^2 is nearly

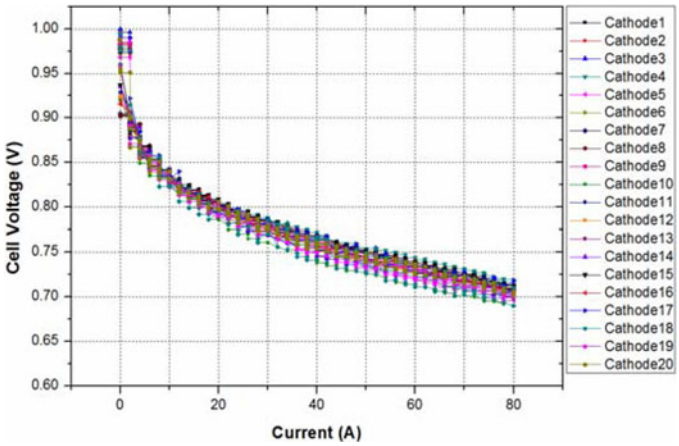

Fig. 7. Cell voltage difference utilizing H_2/air with the 1-kW class PEM fuel cell 20-cell stack on an active area of 150 cm^2.

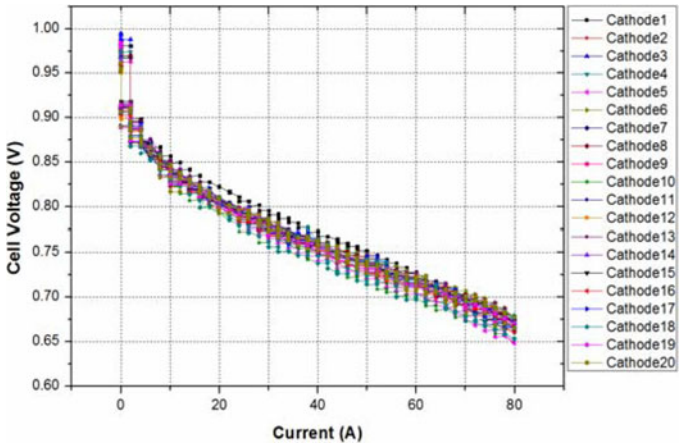

Fig. 8. Cell voltage difference utilizing H_2/O_2 with the 1-kW class PEM fuel cell 20-cell stack on an active area of 150 cm^2.

four times more than those of a basic unit of 25 cm^2. The parallel scaled-up by increasing active area has the advantage of easy assembly and maintenance with very few cells, but the disadvantages of safety and bulky assembly due to too thick power cable because the current of serial scaled-up PEM fuel cell is proportional to the multiple of active area.

As shown in Fig. 4, the 1-kW class PEM fuel cell stack is scaled-up sufficiently by stacking 20 cells in series with an active area of 150 cm^2 in parallel while limiting to the maximum current of 80 A and maintaining both durability and balance between 20 cells. The scale-ups in series by stacking cells and in parallel by increasing active area depend on the voltage and current requirements for specific applications. The scale-up of stacking 20 cells in series with an active area of 150 cm^2 each provides durability and balance between the cells while the stack can be operated in a nominal current and voltage range of 40–80 A and 15–12 V, respectively, with a maximum nominal power of 1 kW.

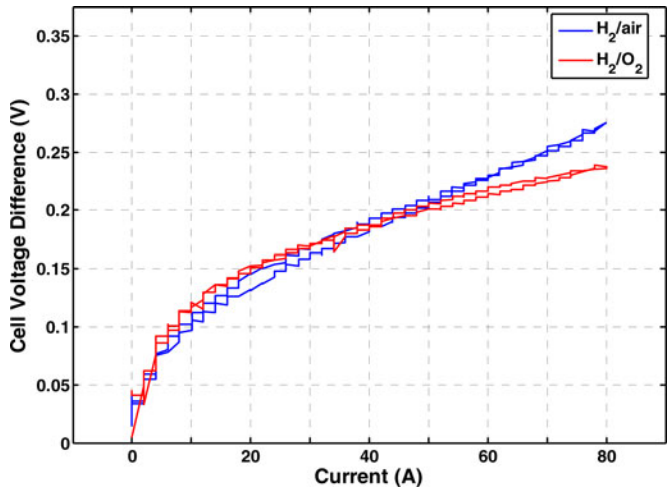

Fig. 9. Comparison of cell voltage differences utilizing H_2/air and H_2/O_2 with the 1-kW class PEM fuel cell 20-cell stack on an active area of 150 cm^2.

C. Characterization of Oxidant

The cell voltages of 20 cells in the 1-kW class PEM fuel cell are shown in Figs. 7 and 8 utilizing H_2/air and H_2/O_2, respectively, while the load currents were controlled according to predefined schedules given in Fig. 3. The cell voltages with H_2/O_2 are similar as than those with H_2/air at the activation loss and the ohmic resistance loss regions in the current range of 0–50 A; however, stack voltage and power with H_2/O_2 is higher by approximately 0.05 V than those with H_2/air at the mass transport loss region in the current range over 50 A.

The *V–I* curves in the ohmic resistance and mass transport regions are shifted downward with decreasing O_2 mole fraction in the cathode feed. O_2 is consumed by reaction at the CL, driving both convective and diffusive flows across the GDL. Convection is driven by a pressure difference resulting from a reduction in molar concentration associated with O_2 consumption at the catalyst. Diffusion across the cathode GDL is driven by the concentration difference between the gas flow channel and the CL. The proton current is driven by the chemical potential difference between the chemical potential of hydrogen at the anode and cathode CLs [7].

The switch from pure O_2 to air as oxidant has a large effect on the utilization of the catalyst in a PEM fuel cell. The differences between maximum and minimum cell voltages at a current utilizing H_2/air and H_2/O_2 with the 1-kW class PEM fuel cell stack are shown and compared in Fig. 9. As current exceeds 50 A, cell voltage difference with H_2/O_2 becomes smaller than that with H_2/air. The entire width of the catalyst under the land was active when pure O_2 was fed to the PEM fuel cell, but only a limited part of the CL was active when air was fed instead [7]. O_2 must be transported through the GDL in both the transverse and lateral directions to the CL. Because the distance for diffusion under the land is generally greater than the thickness of the GDL, we anticipate significant diffusional limitations for O_2 to reach the cathode CL further under the land when the O_2 is diluted by nitrogen (N_2) [11].

Mass transport limitations with an air as oxidant fed cathode were most important at large overpotential, corresponding to

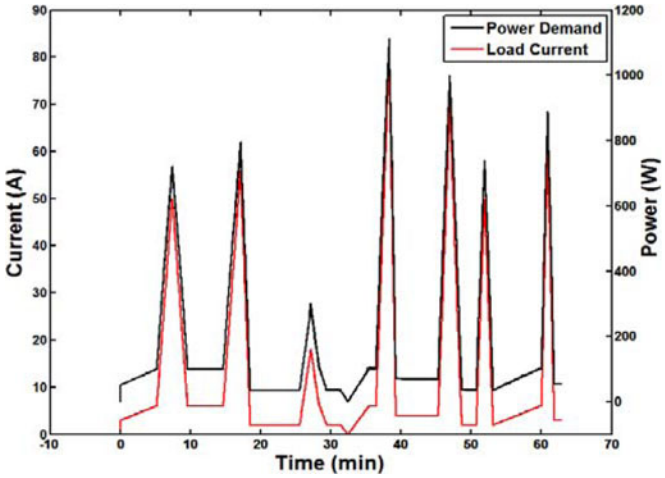

Fig. 10. Power demand profile and controllable load current with the 1-kW class PEM fuel cell 20-cell stack on an active area of 150 cm^2.

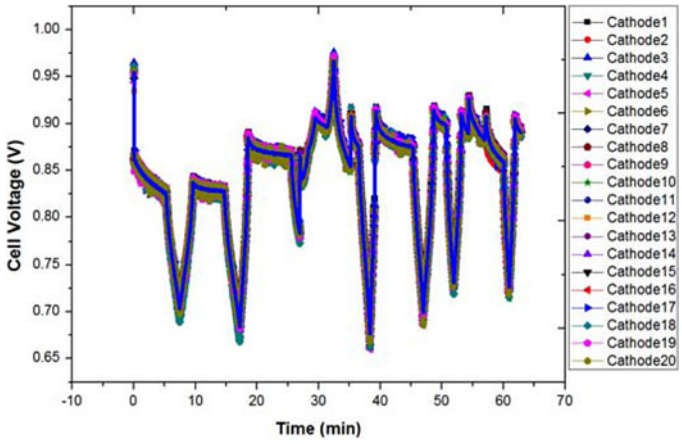

Fig. 12. Responding cell voltages of 20 cells and one-twentieth of the stack voltage utilizing H_2/air with the 1-kW class PEM fuel cell 20-cell stack on an active area of 150 cm^2.

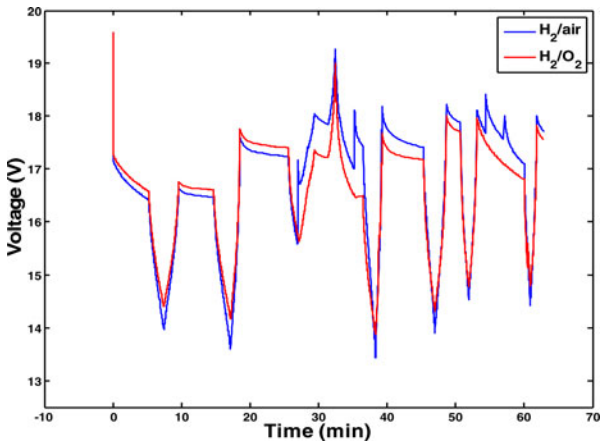

Fig. 11. Changes of the responding stack voltage according to the power demand and load current utilizing H_2/air and H_2/O_2 with the 1-kW class PEM fuel cell 20-cell stack on an active area of 150 cm^2.

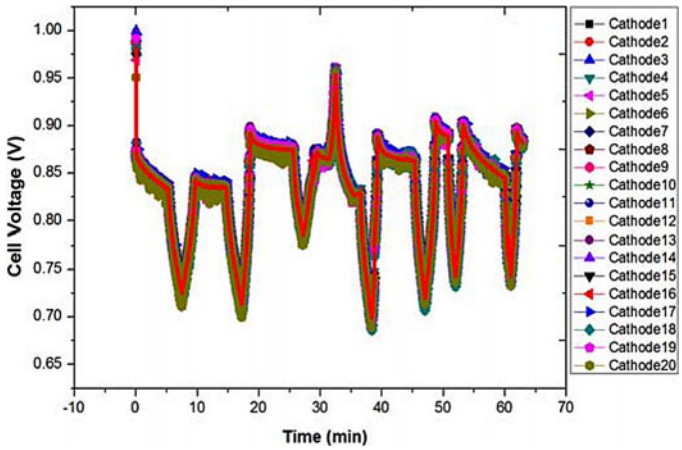

Fig. 13. Responding cell voltages of 20 cells and one-twentieth of the stack voltage utilizing H_2/O_2 with the 1-kW class PEM fuel cell 20-cell stack on an active area of 150 cm^2.

high load resistance [21]. The air and O_2 in the 1-kW class PEM fuel cell stack are characterized through the comparison of cell voltage differences utilizing H_2/air and H_2/O_2.

D. Response Characteristics of the 1-kW Stack

The first task of the 1-kW class PEM fuel cell stack is designed to characterize the response to operation under conditions that are representative of the real power demands. To compare the response characteristics with the reactants of H_2/air and H_2/O_2, the power demand profile can be reasonably determined with a variety of low and high peak, as shown in Fig. 10. This is an important measure to assess the response characteristics of the 1-kW class PEM fuel cell stack, but do not compare with the steady-state data of 5 s shown in Fig. 4. The power demand profile is transformed to controllable load current.

The responding stack voltage of the 1-kW class PEM fuel cell stack is changed according to the change of the power demand and load current with H_2/air and H_2/O_2, as shown in Fig. 11. The responding stack voltage variation is analyzed as follows: the responding stack voltage with H_2/O_2 is higher than that with H_2/air in the time and load current ranges of 0–26 min and 30–80 A, respectively, while the responding stack voltage with H_2/O_2 is less than that with H_2/air in the time and load current ranges of 26–80 min and 0–30 A, respectively. As time passes, the transport resistance across the GDL is increased by dilution of H_2/O_2 concentrations with water at higher temperature; therefore, the stack voltage with H_2/O_2 is higher than H_2/air in the time range of 19–25 min but vice versa 48–51 min even at the same current of approximately 2 A [7]. The voltage with H_2/air and H_2/O_2 are responded and synchronized with the load current and achieved the power demand. There are some voltage spikes in order to test the immediate response to the sudden change of power demand. We confirmed that multiplication of the voltage and the load current is the same as the power demand.

The responses, that is, cell voltages of 20 cells including one-twentieth of the responding stack voltage with the 1-kW class

PEM fuel cell stack with an active area of 150 cm^2 utilizing H_2/air and H_2/O_2, are shown in Fig. 12 and 13 Both cell voltages with H_2/air and H_2/O_2 follow well the one-twentieth of the corresponding stack voltage with H_2/air and H_2/O_2 with the small difference. These operational responses provide both durability and balance in the 1-kW class PEM fuel cell stack with 20 cells.

IV. Conclusion

In this paper, scale-up, oxidant, and response characteristics of the 1-kW class 20-cell PEM fuel cell stack with an active area of 150 cm^2 are investigated experimentally. To characterize the scale-up procedure of PEM fuel cells, a basic unit cell with an active area of 25 cm^2, a serial scaled 4-cell stack with an active area of 25 cm^2, and a parallel scaled-up single cell stack with an active area of 100 cm^2, and serial and parallel scaled-up 1-kW class 20-cell stack with an active area of 150 cm^2, are subsequently fabricated and evaluated. All fuel cells have novel serpentine flow fields with subchannels and by-passes to promote under-rib convection.

To achieve the 1-kW class PEM fuel cell, there are two approaches of a serial scaled-up by stacking cell and a parallel scaled-up by increasing active area. The maximum cell voltage and the maximum power of the serial scaled 4-cell stack are nearly four times more than those of the basic unit cell. The maximum current and the maximum power of a parallel scaled-up single cell of 100 cm^2 are nearly four times more than those of a basic unit of 25 cm^2. The 1-kW class PEM fuel cell stack is scaled up sufficiently by stacking 20 cells in series with an active area of 150 cm^2 in parallel. The polarization and power curves of the 1-kW class PEM fuel cell stack with the reactants H_2/air and H_2/O_2 are characterized in four regions through the comparisons of the stack voltage and power.

The cell voltages of 20 cells in the 1-kW class PEM fuel cell stack are compared with H_2/air and H_2/O_2, respectively, while the load currents were controlled according to predefined schedules. The entire width of the catalyst under the land was active when pure O_2 was fed to the PEM fuel cell, but only a limited part of the CL was active when air was fed instead. O_2 must be transported through the GDL in both the transverse and lateral directions to the CL. Because the distance for diffusion under the land is generally greater than the thickness of the GDL, we anticipate significant diffusional limitations for O_2 to reach the cathode CL further under the land when the O_2 is diluted by N_2. The air and O_2 in the 1-kW class PEM fuel cell stack are characterized through the comparison of cell voltage differences utilizing H_2/air and H_2/O_2 for operating in connection with water PEM electrozer.

To compare the response characteristics with the reactants of H_2/air and H_2/O_2, the power demand profile can be reasonably determined with a variety of low and high peak. The responding stack voltage variation is analyzed, in four regions shown in Fig. 4. The responding stack voltage with H_2/O_2 is clearly higher than that with H_2/air in the high external load current range over 30 A of mass transport loss region. However, the responding stack voltage with H_2/O_2 is similar or less than that with H_2/air in the low external load current range under 30 A of activation loss and ohmic resistance loss regions. Both cell voltages with H_2/air and H_2/O_2 follow well the one-twentieth of the responding stack voltage with H_2/air and H_2/O_2 with the small difference. These operational results would help us advance to the necessary balance between the performances of 1-kW PEM fuel cell stack with 20 cells without cell failure for operating energy storage of smart grid.

References

[1] F. Barbir, *PEM Fuel Cells: Theory and Practice*, 1st ed. New York, NY, USA: Elsevier, 2005, pp. 10–17.

[2] M. W. Ellis, M. R. Von Spakovsky, and D. J. Nelson, "Fuel cell systems: Efficient, flexible energy conversion for the 21st century," *Proc. IEEE*, vol. 89, no. 12, pp. 1808–1818, Dec. 2001.

[3] J. M. Corrêa, A. A. Farret, L. N. Canha, and M. G. Simões, "An electrochemical-based fuel-cell model suitable for electrical engineering automation approach," *IEEE Trans. Energy Convers.*, vol. 51, no. 5, pp. 1103–1112, Oct. 2004.

[4] F. Gao, M. G. Simões, and A. Miraoui, "PEM fuel cell stack modeling for real-time emulation in hardware-in-the-loop applications," *IEEE Trans. Ind. Electron.*, vol. 26, no. 1, pp. 184–194, Mar. 2011.

[5] K.-S. Choi, B.-G. Kim, K. Park, and H.-M. Kim, "Current advances in polymer electrolyte fuel cells based on the promotional role of under-rib convection," *Fuel Cells*, vol. 12, pp. 908–938, 2012.

[6] A. S. Samosir, M. Anwari, and A. H. M. Yatim, "A simple PEM fuel cell emulator using electrical circuit model," in *Proc. IEEE Power Electron. Soc. Gen. Meet.*, Singapore, Oct. 2010, pp. 881–885.

[7] J. Benziger, E. Kimball, R. Mejia-Ariza, and I. Kevrekidis, "Oxygen mass transport limitations at the cathode of polymer electrolyte membrane fuel cells," *AIChE J.*, vol. 57, pp. 2505–2517, 2011.

[8] B. Fang, J. H. Kim, C. Lee, and J.-S. Yu, "Hollow macroporous core/mesoporous shell carbon with a tailored structure as a cathode electrocatalyst support for proton exchange membrane fuel cells," *Phys. Chem. C*, vol. 112, pp. 639–645, 2008.

[9] K.-S. Choi, H.-M. Kim, and S.-M. Moon, "Numerical studies on the geometrical characterization of serpentine flow-field for efficient PEMFC," *Int. J. Hydrog. Energy*, vol. 36, pp. 1613–1627, 2011.

[10] J. H. Nam, K. J. Lee, S. Sohn, and C. H. Kim, "Multi-pass serpentine flow-fields to enhance under-rib convection in polymer electrolyte membrane fuel cells: design and geometrical characterization," *J. Power Sources*, vol. 188, pp. 14–23, 2009.

[11] K.-S. Choi, H.-M. Kim, and S.-M. Moon, "An experimental study on the enhancement of the water balance, electrochemical reaction and power density of the polymer electrolyte fuel cell by under-rib convection," *Electrochem. Commun.*, vol. 13, pp. 1387–1390, 2011.

[12] K.-S. Choi, B.-G. Kim, K. Park, and H.-M. Kim, "Flow control of under-rib convection enhancing the performance of proton exchange membrane fuel cell," *Comput. Fluids*, vol. 69, pp. 81–92, 2012.

[13] B. Lee, K. Park, and H.-M. Kim, "Numerical optimization of flow field pattern by mass transfer and electrochemical reaction characteristics in proton exchange membrane fuel cells," *Int. J. Electrochem. Sci.*, vol. 8, pp. 219–234, 2013.

[14] T. Malkow *et al.*, *PEFC Power Stack Performance Testing Procedure: Measuring Voltage and Power as Function of Current Density Following a Dynamic Profile Versus Time, Dynamic Load Cycling Aging Test. Test Module PEFC ST 5-3*, European Union, 2010.

[15] X.-D. Wang *et al.*, "An inverse geometry design problem for optimization of single serpentine flow field of PEM fuel cell," *Int. J. Hydrog. Energy*, vol. 35, pp. 4247–4257, 2010.

[16] J. Benziger, E. Chia, E. Karnas, J. Moxley, C. Teuscher, and I. Kevrekidis, "The stirred tank reactor polymer electrolyte membrane fuel cell," *AIChE J.*, vol. 50, pp. 1889–1900, 2004.

[17] Y. Hou, "A study on polarization hysteresis in PEM fuel cells by galvanostatic step sweep," *Int. J. Hydrog. Energy*, vol. 36, pp. 7199–7206, 2011.

[18] T. Zawodzinski *et al.*, "Water-uptake by and transport through Nafion 117 membranes," *J. Electrochem. Soc.*, vol. 140, pp. 1041–1047, 1993.

[19] S. J. Lee *et al.*, "Effects of Nafion impregnation on performances of PEMFC electrodes," *Electrochim. Acta*, vol. 43, pp. 3693–3701, 1998.

[20] F. Laurencelle *et al.*, "Characterization of a Ballard MK5-E proton exchange membrane fuel cell stack," *Fuel Cells*, vol. 1, pp. 66–71, 2001.
[21] W. Sun, B. A. Peppley, and K. Karan, "Modeling the influence of GDL and flow-field plate parameters on the reaction distribution in the PEMFC cathode catalyst layer," *J. Power Sources*, vol. 144, pp. 42–53, 2005.

Kap-Seung Choi (M'13) received the B.S., M.S., and Ph.D. degrees in mechanical engineering from Inje University, Gyeongnam, Korea, in 2004, 2006, and 2011, respectively.

Since 2013, he has been an Assistant Professor in Automobile Engineering at Tongmyong University, Busan, Korea. His research interests include fuel cell systems dedicated to automotive applications; system modeling, hardware-in-the-loop applications, and energy optimization of these systems; and fuel-cell system diagnosis.

Dr. Choi is a member of IEEE Power and Energy Society.

Jiwoong Ahn (M'13) was born in Seoul, Republic of Korea, in 1989. He is currently working toward the B.S. degree in mechanical and automotive engineering at Inje University, Gimhae, Republic of Korea.

From 2009 to 2010, he was an Army Soldier and received full-time discharge in December 2010. Since 2013, he has been a Researcher in the Power System & Sustainable Energy Laboratory, Inje University. His research interests include ocean kinetic energy harvester based on ionic polymer metal composite.

Mr. Ahn is a member of IEEE Power and Energy Society.

Jungkoo Lee (M'13) was born in Nonsan, Korea, in 1988. He is currently working toward the B.S. degree in mechanical and automobile engineering at Inje University, Busan, Korea.

Since 2013, he has been a Researcher in the Power System & Sustainable Energy Laboratory, Inje University. His research interests include fuel cells and hydrogen engine.

Mr. Lee is a member of IEEE Power and Energy Society.

Nguyen Duy Vinh (M'13) received the B.S. and M.S. degrees in mechanical engineering from the Hanoi University of Science and Technology, Hanoi, Vietnam, in 2007 and 2011, respectively. Since 2013, he has been working toward the Ph.D. degree in the Power System & Sustainable Energy Lab, Inje University, Busan, Korea.

From 2007 to 2012, he was a Researcher at the Lab of Internal Combustion Engine, Hanoi University of Science and Technology. His research interests include the power system, fuel cell, electric vehicle, renewable energy, and engine emissions.

Mr. Vinh is a member of IEEE Power and Energy Society.

Hyung-Man Kim (M'13) received the B.S. and M.S. degrees in mechanical engineering from Seoul National University, Seoul, Korea, in 1987 and 1992, respectively, and the Ph.D. degree in aeronautical and astronautical engineering from the University of Tokyo, Tokyo, Japan, in 1997.

Since March 1997, he has been a Full Professor in Mechanical and Automotive Engineering at Inje University, Busan, Korea, where he has been the Director of the National Leading Research Laboratory since 2009. He is also the Editor of the *International Journal of Automotive Technology*. His research interests include integration and control of regenerative fuel cell with photovoltaic cell, renewable energy of ocean kinetic energy harvester, distributed generation, smart grid, and sustainable energy for global environment.

Dr. Kim is a member of IEEE Power and Energy Society.

Kiwon Park (M'07) was born in Busan, Republic of Korea, in 1977. He received the Ph.D. degree in biomedical engineering from the South Dakota School of Mines and Technology, Rapid City, SD, USA, in 2011.

Since 2012, he has been a Research Professor at the Power System & Sustainable Energy Lab, Inje University, Busan. His research interests include regenerative fuel cell system, energy harvesting utilizing electroactive polymers, and sensors and devices in mechanical and biomedical engineering applications.

Dr. Park is a member of IEEE Power and Energy Society.

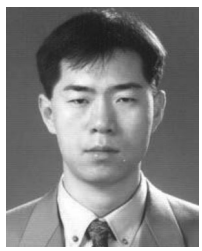

Gunyong Hwang (M'06) received the Ph.D. degree in mechanical design engineering from Busan National University, Busan, Korea, in 2003.

Since 2002, he has been a Full Professor in the Department of Green Automobile Engineering at Youngsan University, Yangsan-si, Korea, where he has been in charge of the Product Development Laboratory since 2006. His research interests include motors in electric automobile applications, decarbonization energy harvesting, and fuel cell systems.